


Article

Considerations About Bi and Pb in the Crystal Structure of Cu-Bearing Tourmaline

Andreas Ertl ^{1,*} and Peter Bačík ² ¹ Institut für Mineralogie und Kristallographie, Universität Wien, Althanstrasse 14, 1090 Wien, Austria² Department of Mineralogy and Petrology, Faculty of Natural Sciences, Comenius University in Bratislava, Ilkovičova 6, 842 15 Bratislava, Slovakia; peter.bacik@uniba.sk

* Correspondence: andreas.ertl@a1.net

Received: 8 July 2020; Accepted: 7 August 2020; Published: 10 August 2020



Abstract: Copper- and Mn-bearing elbaitic tourmaline (“Paraíba tourmaline”) sometimes contains significant amounts of Pb and Bi. Their position in the tourmaline crystal structure was studied with correlation analysis and bond valence calculations. Correlations between the F content and the X-site charge allow predicting the X-site occupancy. Three sets of tourmaline analyses were studied: (1) Pb-rich tourmalines from the Minh Tien pegmatite, Vietnam; (2) Cu-, Pb- and Bi-bearing tourmalines from the Mulungu mine, Brazil; (3) Cu- and Bi-bearing tourmalines from the Alto dos Quintos mine, Brazil. Two correlations were plotted: (1) the charge by considering only Na¹⁺, Ca²⁺ and K¹⁺; (2) the charge by adding Pb²⁺ and Bi³⁺ to the X-site charge. When plotting correlations for the Minh Tien tourmalines, the correlation significantly improves by adding Pb²⁺ to the X site. For the Alto dos Quintos tourmalines, only a slight increase of the correlation coefficient is observed, while such a correlation for tourmalines from Mulungu interestingly shows a slight decrease of the correlation coefficient. Bond valence calculations revealed that Bi³⁺ and Pb²⁺ can indeed occupy the X site via BiLi(NaAl)_{−1}, PbLi(NaCu)_{−1} and possibly PbCu(NaAl)_{−1} substitutions as seen in the investigated tourmaline samples. At the Y site, Pb⁴⁺ can be substituted via PbLi(AlCu)_{−1}, and Pb^VO(Al^VOH)_{−1}, while Bi⁵⁺ does not have any stable arrangement in Cu-bearing fluor-elbaite. The occurrence of Pb⁴⁺ at the Y site could be one explanation for the results of the correlations of the Mulungu tourmalines. Another explanation could be that during the tourmaline crystallization some additional Bi and Pb came into the pegmatitic system and hence disturbed the correlation between the average X-site charge and the F content. Further plots of such correlations in “Paraíba tourmaline” samples might also help to distinguish between the worldwide localities of these rare and sought-after tourmalines.

Keywords: tourmaline; bismuth; lead; crystal structure; correlation analysis; bond valence calculation

1. Introduction

In tourmaline, with the general structural formula $XY_3Z_6(BO_3)_3T_6O_{18}V_3W$, the individual structural sites can be occupied mainly by the following cations: X site = Na, Ca, Pb, K, □ (vacancy); Y site = Li, Mg, Fe²⁺, Mn²⁺, Cu²⁺, Al, Cr³⁺, V³⁺, Fe³⁺; Z = Al, Mg, Fe²⁺, Fe³⁺, V³⁺, Cr³⁺; T site = Si, Al, B; V = OH[−], O^{2−}; W = OH[−], F[−], Cl[−], O^{2−} [1–20]. The crystal structure of natural Cu-bearing tourmaline was described by [18,21–23]. No Bi and/or Pb were described in these elbaitic tourmalines, which were found in granitic pegmatites in Brazil and Mozambique. The first crystal structure of a tourmaline sample (Li-bearing olenite; Cu below the detection limit) with significant amounts of Pb (1640 ppm) and Bi (143 ppm) was described from a pegmatitic “mushroom” tourmaline from Myanmar by [24]. They were the first authors who assigned these small amounts of Pb and Bi to the X site, just because no phases other than tourmaline have been observed on their back-scattered electrons (BSE) pictures.

The chemistry of natural Cu-bearing tourmalines with significant amounts of Bi (up to ~0.5–0.8 wt % Bi₂O₃) was described by [25–28]. The highest amount of Bi (~1.5 wt % Bi₂O₃) in Cu-bearing tourmaline was described by [29]. Tourmalines with up to ~0.5 wt % Bi₂O₃, but without significant amounts of Cu were described by [30] from a granitic pegmatite in Zambia.

The chemistry of natural Cu-bearing tourmalines with significant amounts of Pb (up to ~0.4 wt % PbO) was described by [28]. Tourmalines (fluor-liddicoatite; Cu below the detection limit) with up to ~0.6 wt % PbO were described by [31] from a granitic pegmatite in Madagascar. Even more Pb (up to ~5.9–17.5 wt % PbO) was described in tourmalines (Cu below the detection limit) from a granitic pegmatite in Vietnam by [32–34].

Already [35] showed in an evaluation of ~600 chemical analyses of different tourmalines that samples with >0.5 X-site vacancies exhibit little or no F. A positive correlation with $R^2 \approx 1$ between the F content and the X-site charge of tourmaline samples from one granitic pegmatite was described for the first time by [36]. These authors plotted the average X-site charge (of the X-site occupants Na and Ca; K was at the detection limit) against the F content of the W site. Their studied samples (tourmalines of the fluor-elbaite–rossmanite solid solution series) came from a pegmatite from Wolkenburg near Limbach-Oberfrohna, Saxony, Germany. Subsequently, more such correlations were observed in other pegmatites, like the Himalaya mine pegmatite in Mesa Grande, Ca, USA [37]. The average charge of the observed X-site occupants (Na, Ca and K) of different tourmalines (oxy-schorl, fluor-elbaite, elbaite) from this pegmatite were plotted against the F content ($R^2 \approx 1$; [37]). Due to the such good correlations between the average charge of the X-site occupants and the F content in tourmalines from the same pegmatite, we tried to find out if there are some indications for Pb²⁺ and Bi³⁺ to occupy the X site in Cu-bearing tourmaline.

2. Theory and Correlations

In contrast to the elements of the d-block, such as the transition metals, the heavier p-block metals favor low oxidation states. Especially all the heavier members favor oxidation numbers two fewer than the group oxidation number. For example, as the heaviest member of group 15 (V), bismuth favors Bi³⁺. The same trend is observed for Pb. Bismuth has the electronic configuration [Xe]4f¹⁴5d¹⁰6s²6p³ and of the major oxidation states of bismuth (+3 and +5), Bi³⁺ is the most common and stable oxidation state [38]. There is an increasing stability of lower oxidation states for heavier elements. The vast bulk of aqueous bismuth chemistry is dominated by Bi³⁺ and Pb²⁺, particularly in those environments of geological relevance [39]. Hence, Bi and Pb usually occur in nature as Bi³⁺ and as Pb²⁺ in minerals. Their effective ionic radii ([9]Bi³⁺: ~1.23 Å, [9]Pb²⁺: 1.35 Å; [40]) fit well for the tourmaline X site, compared with the radii for Na¹⁺ (1.24 Å), Ca²⁺ (1.18 Å), and K¹⁺ (1.55 Å). Rarely were minerals described which contain Bi⁵⁺ and Pb⁴⁺. Such minerals can only be found in an oxidative environment.

To learn more about the influence of Pb²⁺ at the tourmaline X site to the correlation between the X-site charge and the F content, we plotted a representative amount of unusual Pb-rich tourmaline samples (up to ~8.6 wt % PbO; [33]). For a first correlation, the charge by considering only Na¹⁺, Ca²⁺ and K¹⁺ was plotted ($R^2 = 0.07$; Figure 1). For a second correlation also Pb²⁺ was included for the calculation of the X-site charge ($R^2 = 0.80$; Figure 2). This result shows that also the charge of heavy elements (like Pb²⁺ and Bi³⁺) influences the correlation between the average X-site occupation and the F content. One explanation that the correlation in Figure 2 is not even better, might be because the matrix effects (because of the unusual high Pb content in tourmaline) during electron microprobe analyses, have an increasingly negative effect on the total sum, which goes down to ~96% in tourmaline samples with relatively high amounts of PbO. Indeed, we utilized an increase in R^2 with inclusion of Pb²⁺ in the X-site charge over a certain range (Pb < 0.30 atoms per formula unit (apfu); $R^2 = 0.85$).

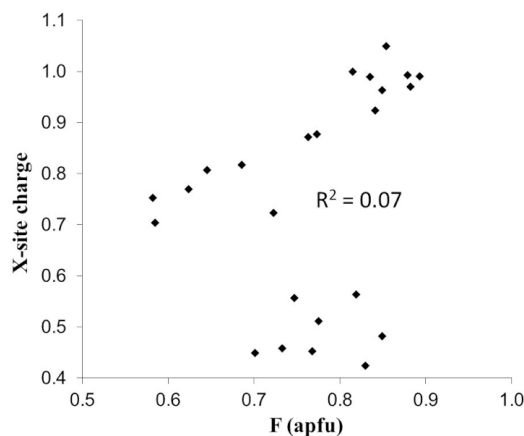


Figure 1. Correlation between the average X-site charge (Na^{1+} , Ca^{2+} , K^{1+} , without Pb^{2+}) in Pb-rich tourmalines from the Minh Tien pegmatite, Luc Len district, Vietnam (samples from [33]).

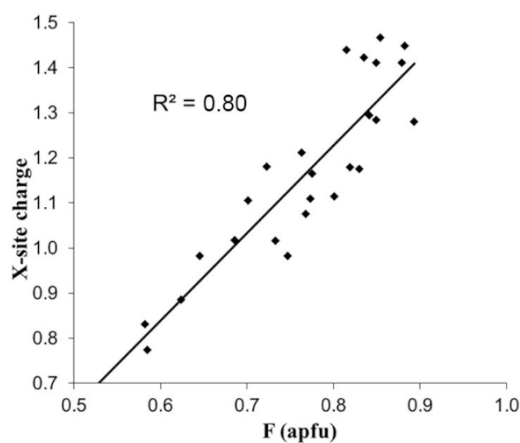


Figure 2. Correlation between the average X-site charge (Na^{1+} , Ca^{2+} , K^{1+} , Pb^{2+}) in Pb-rich tourmalines from the Minh Tien pegmatite, Luc Len district, Vietnam (samples from [33]).

Copper-bearing tourmalines (fluor-elbaite, elbaite) from the Mulungu mine (Capoeira 2 pegmatite) in the Rio Grande do Norte State, Brazil, contain significant amounts of Bi (up to 0.81 wt % Bi_2O_3) and smaller amounts of Pb (up to 0.23 wt % PbO) as was described by [26]. We calculated the Li_2O content (difference to a completely with cations filled Y site), the B_2O_3 content (stoichiometric content with $\text{B} = 3.00$ apfu and the H_2O content ($\text{F} + \text{OH} = 4$ apfu) for every tourmaline sample. Then, we plotted the X-site charge against the F content of all samples. As first, we plotted only the charge of Na, Ca and K (Figure 3). The result is a very good positive correlation with $R^2 = 0.98$. As a next step, we added to the average X-site charge (Na, Ca, K) also the charge of the small amounts of Bi^{3+} and Pb^{2+} . The result of the new correlation (Figure 4) is getting worse ($R^2 = 0.95$). We also checked the correlation in the case of adding only either Bi or Pb separately. The R^2 value gets also worse by including either Bi or Pb.

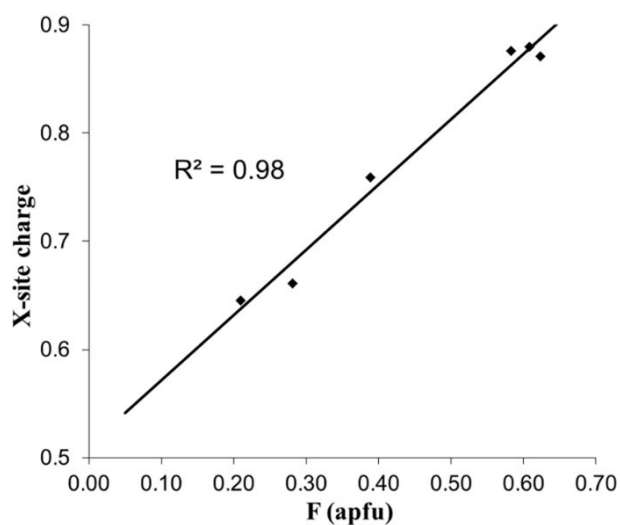


Figure 3. Correlation between the average X-site charge (only Na^{1+} , Ca^{2+} , K^{1+}) in Cu-bearing tourmalines from the Mulungu mine, Rio Grande do Norte, Brazil (samples from [26]).

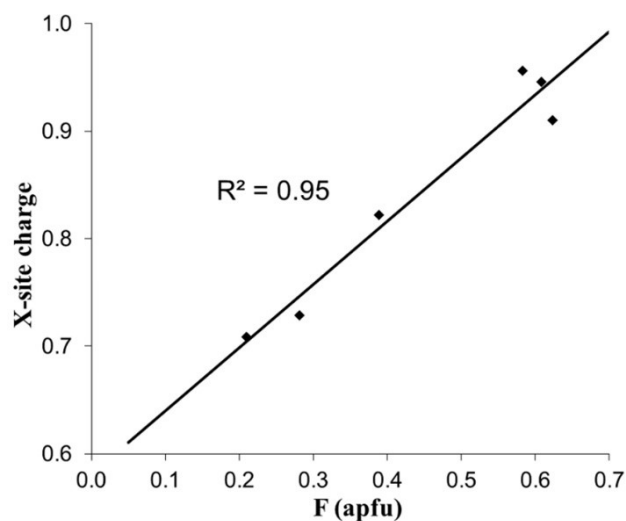


Figure 4. Correlation between the average X-site charge (Na^{1+} , Ca^{2+} , K^{1+} , Bi^{3+} , Pb^{2+}) in Cu-bearing tourmalines from the Mulungu mine, Rio Grande do Norte, Brazil (samples from [26]).

We also plotted tourmaline samples from the Alto dos Quintos mine, which is also in the Rio Grande do Norte State, Brazil [22,27,41,42] (for all samples the light elements B, Li, H were calculated as described above). These samples contain up to 0.49 wt % Bi_2O_3 , but almost no Pb (≤ 0.02 wt % PbO) [27]. Again, we first plotted only the charge of Na, Ca and K (Figure 5). The result is a very good positive correlation with $R^2 = 0.91$ (Figure 5). For the following plot (Figure 6) we added also the charge of the small amounts of Bi^{3+} . This time the correlation is even getting better ($R^2 = 0.94$; Figure 6).

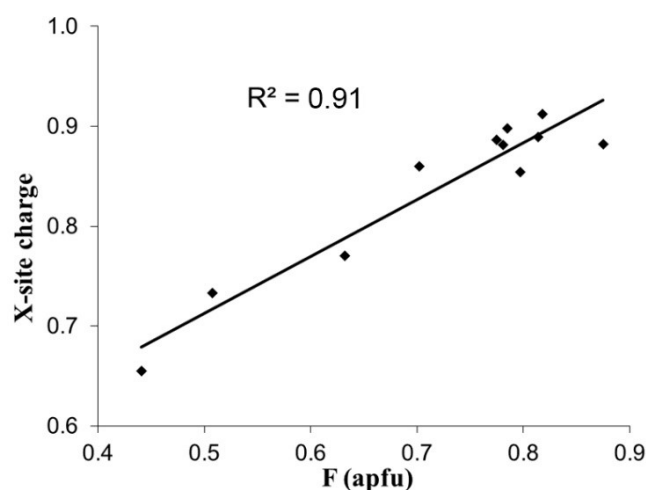


Figure 5. Correlation between the average X-site charge (only Na^{1+} , Ca^{2+} , K^{1+}) in Cu-bearing tourmalines from the Alto dos Quintos mine, Rio Grande do Norte State, Brazil (samples from [22,27,41,42]).

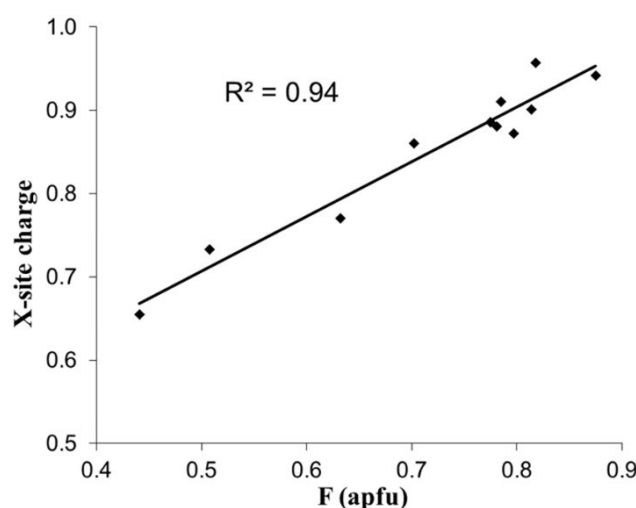


Figure 6. Correlation between the average X-site charge (Na^{1+} , Ca^{2+} , K^{1+} , Bi^{3+}) in Cu-bearing tourmalines from the Alto dos Quintos mine, Rio Grande do Norte State, Brazil (samples from [22,27,41,42]).

It should be mentioned that a recent X-ray absorption fine structure (XAFS) study on the location of Cu and Mn in fluor-elbaite with $\text{CuO} = 1.08 \text{ wt } \%$ and $\text{MnO}_{\text{total}} = 1.58 \text{ wt } \%$ from the Alto dos Quintos mine was published by [42]. These authors described a Mn K-edge XANES spectrum of that Cu- and Mn-bearing tourmaline together with spectra of MnO and Mn_2O_3 . As the edge position for that tourmaline was lying between those of the standard oxides, [42] suggested a mixed valence state of Mn. They obtained a population of $\text{Mn}^{2+}/(\text{Mn}^{2+} + \text{Mn}^{3+}) = 0.6$ by its edge energy relative to those of the standard oxides. Hence, a relatively high amount of 40% of the total Mn in this Cu-bearing tourmaline was oxidized to Mn^{3+} . No further known studies exist, which determined the valence state of Mn and Fe in any of the Cu-bearing tourmalines.

3. Bond Valence Calculations

Bond-length calculations are based on the following equation:

$$d_{ij} = R_0 - b \ln v_{ij}, \quad (1)$$

where d_{ij} is the bond length (in Å) between the two given atoms, the bond valence (v_{ij}) measures bond strength (in vu—valence units), R_0 is the length of a single bond (for which $v_{ij} = 1$ vu), and b is the universal parameter for each bond [43]. This is based on the following:

- (1) The evaluation of published bond valence parameters for 128 cations bonded to oxygen, using a very large set of bond lengths that have undergone rigorous filtering;
- (2) The investigation of many alternative algebraic forms of the bond valence–bond length relation;
- (3) The evaluation of different fitting methods used in the derivation of bond valence parameters;
- (4) The determination of new bond valence parameters for 135 cations bonded to oxygen, the R_0 and b values for each cation from the list of [44] were used. Bond lengths (Table 1) were calculated for all possible valence states of Pb and Bi and for both X- and Y-site coordination.

Table 1. Calculated bond lengths (in Å) of various Bi and Pb cations for Y- and X-site coordination in tourmaline and comparison to the “Goldilocks zone” of stable bond lengths for each site as defined by [45]. Bond lengths of stable bonds are highlighted in bold.

Element	Bond Length [Å]	
	Octahedral Sites	X Site
Bi ³⁺	2.3376	2.4954
Bi ⁵⁺	2.1389	2.2966
Pb ¹⁺	2.8240	3.0032
Pb ²⁺	2.5176	2.6968
Pb ³⁺	2.3384	2.5176
Pb ⁴⁺	2.1695	2.2831
“Goldilocks Zone”		
+10%	2.3335	2.9612
−10%	1.8274	2.4228

Calculated bond lengths were compared to bond lengths typical for the X and Y sites defined as the “Goldilocks zone” of stable bond lengths for each site [45]. It revealed that from all the possibilities only Pb²⁺ and Bi³⁺ could be stable at the X site and Pb²⁺ and Bi³⁺ could substitute cations at the Y site. However, these possibilities should be tested in more detail.

3.1. Pb²⁺ and Bi³⁺ at the X Site

The substitution of Pb²⁺ and Bi³⁺ at the X site can be tested in the structural arrangements at the neighborhood of the X-site cations. The primary arrangement includes Na¹⁺ at the X site, Al³⁺, Cu²⁺ and Li¹⁺ at the Y site, Al³⁺ at the Z site, OH[−] at the V site and F[−] at the W site. It is therefore an arrangement of Cu-bearing fluor-elbaite. Bond valences attached to the graph edges were derived from [46,47] for V- and W-site bonds and [48,49] for Z- and Y-site bonds. X-site valences were calculated from the structure of fluor-schorl [50] and olenite [51] which have the highest Na content at the X site from the whole dataset of [49]. The calculation revealed that the X–O2 bond valence is 0.14 vu (valence units) in both samples, while X–O4 and X–O5 bonds have valences between 0.07 and 0.09 vu. The bond valence sums (BVS) at all sites are equal to the charge of the occupying cations at the Y, V and W sites. The partial BVS at the X site is the sum of 3 × 0.14 vu equal to 0.42 vu. The O2 and O6 oxygens have a BVS of 1, because the remaining 1 vu is reserved for the B–O and T–O bonds. The BVS of the Z sites is not taken into account due to a significant complication of the calculation, but they should always be in the range 0.25–1.0 vu for Al, because otherwise an imbalance of the Z-site bond valence distribution

would be induced. However, it must be considered that the steric and long-range structural effects can absorb small imbalances of the bond valences.

The elbaite structure does not show any extreme bond valence values (Figure 7a). The distribution of X–O2 bond valences reflects a variable Y-site occupation—X–O2 bonds on O2 connecting Al³⁺ and Cu²⁺ are weaker because Al³⁺–O2 and Cu²⁺–O2 took more bond valence than Li¹⁺–O2 bonds. Moreover, a stronger X–O2 bond on O2 between Cu²⁺ and Li¹⁺ allows the stabilization of the local environment by decreasing of bond valence at the Cu²⁺–O2 and Li¹⁺–O2 bonds.

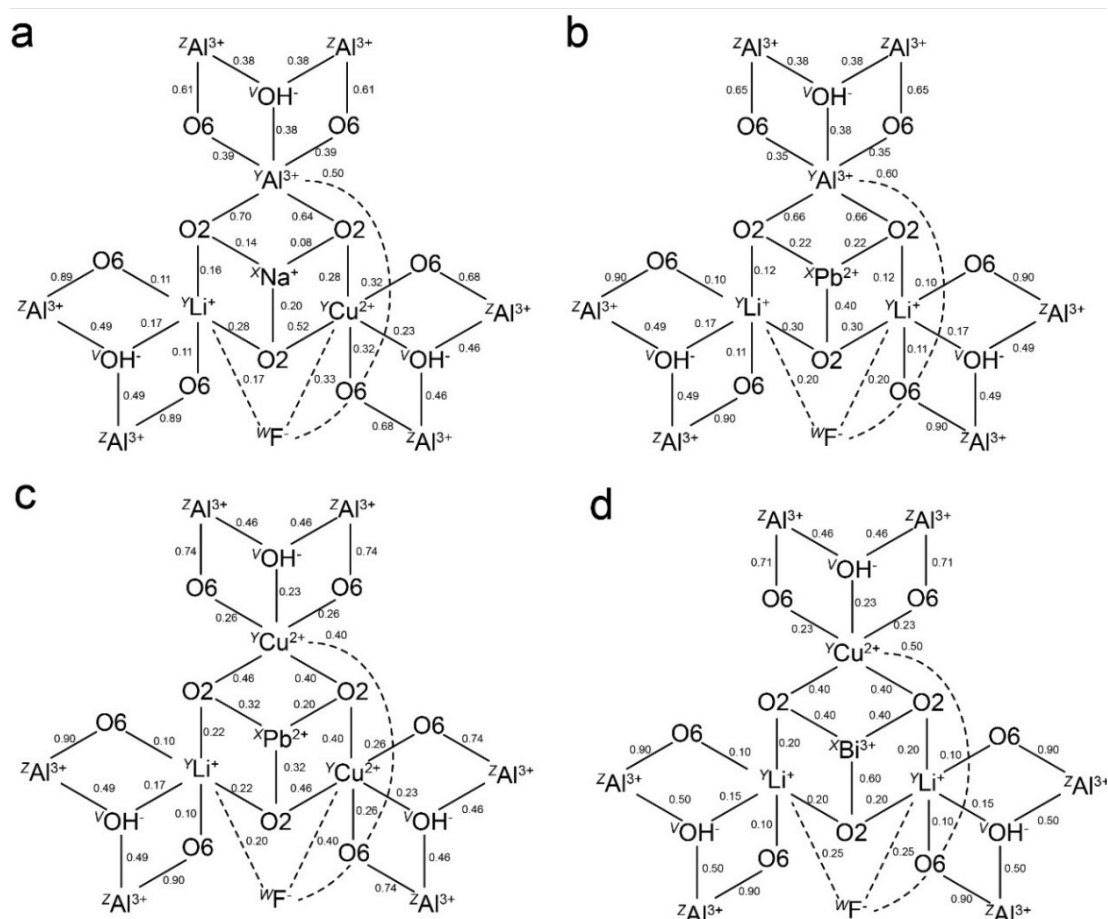


Figure 7. Structural arrangement graphs of the X-site neighborhood in the structure of (a) Cu-bearing fluor-elbaite and arrangements derived from it by (b) Pb²⁺Li¹⁺(Na¹⁺Cu²⁺)_{−1}, (c) Pb²⁺Cu²⁺(Na¹⁺Al³⁺)_{−1} and (d) Bi³⁺Li¹⁺(Na¹⁺Al³⁺)_{−1} substitutions.

First, we considered a substitution of Pb²⁺ for Na¹⁺. This substitution requires charge balancing at the Y site. This can be obtained easily by the substitution of Li¹⁺ for Cu²⁺ resulting in the Pb²⁺-bearing fluor-liddicoatite arrangement (Figure 7b). The distribution of bond valences slightly changed. The X–O2 bond valences are distributed symmetrically with the highest bond valence at the bond of O2 connecting 2 YLi¹⁺ and XPb²⁺ cations. However, all other bond valences indicate a stable arrangement, therefore, Pb²⁺ substitutes relatively easy Na¹⁺ in elbaite and Ca²⁺ in liddicoatitic tourmaline. Another possible substitution involves Cu²⁺ for Al³⁺ at the Y site (Figure 7c). This substitution is similarly plausible as the previous one.

The result of both substitutions can be tested by comparing the Pb²⁺ and Cu²⁺ content. The first PbLi(NaCu)_{−1} substitution results in a negative correlation between Pb and Cu, the second PbCu(NaAl)_{−1} substitution leads to their positive correlation. If there is no correlation, both substitutions can occur simultaneously. Of the studied tourmalines, only the samples from the Mulungu mine contain significant amounts of Cu and Pb to plot a correlation (Figure 8). However, it is not clear

how significant this correlation is, although the R^2 for all available analyses plotted to a value of 0.80. Because of the small number of analyses and the data distribution in this correlation a dominant influence of the $\text{PbCu}(\text{NaAl})_{-1}$ substitution in these samples cannot be proven. When any analysis was removed from this set, R^2 varied between 0.13 and 0.86. Consequently, it cannot be ruled out that the $\text{PbCu}(\text{NaAl})_{-1}$ substitution is present in some samples. However, it must be pointed out that larger datasets are required for a certain determination of the dominant substitution.

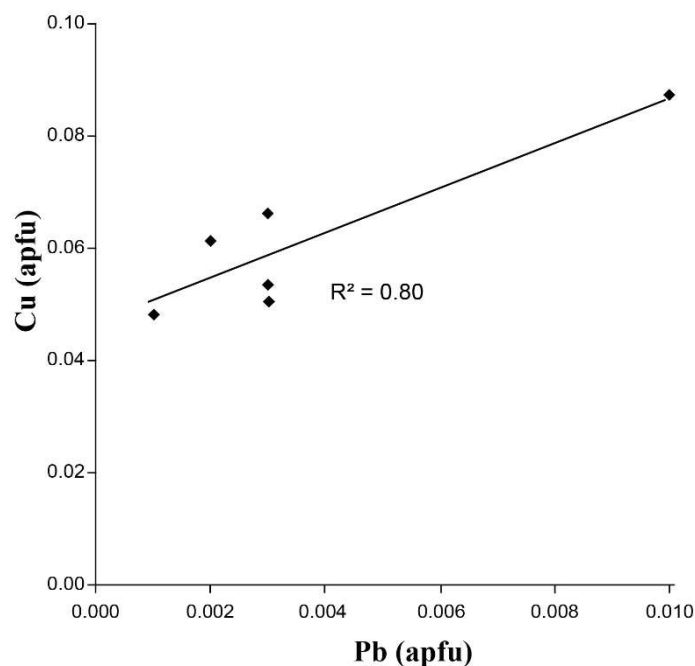


Figure 8. Correlation between Cu^{2+} and Pb^{2+} in Cu-bearing tourmalines from the Mulungu mine, Rio Grande do Norte, Brazil (samples from [26]).

The substitution of Bi^{3+} for Na^{1+} requires a more extensive substitution at the Y site compared to Pb^{2+} . Consequently, if we do not consider a Y-site vacancy or any other more complicated mechanism, there is only one available substitution in contrast to two equally possible substitutions for Pb^{2+} . Starting with a Cu-bearing fluor-elbaite arrangement, Al^{3+} is substituted by Li^{1+} (Figure 7d). The X–O2 bond valences are increased and distributed similarly to the previous arrangement. A calculation of all bonds revealed reasonable bond valences and consequently this substitution is plausible.

A calculation of the structural graphs revealed an increase of the X–O2 bond valence proportional to the X-site cation charge: (1) Na^{1+} has the average X–O2 bond valence of 0.14 vu; (2) Pb^{2+} has the average X–O2 bond valence of 0.28 vu; (3) Bi^{3+} has the average X–O2 bond valence of 0.47 vu. In contrast, an average Y–O2 bond valence has an inverse relationship to the X-site cation charge: (1) Na^{1+} at the X site produces the average Y–O2 bond valence of 0.43 vu; (2) $^{\text{X}}\text{Pb}^{2+}$ results in an average Y–O2 bond valence of 0.36 vu; (3) Bi^{3+} at the X site produces an average X–O2 bond valence of 0.27 vu. This should result in a shortening of the X–O2 bonds and an elongation of the Y–O2 bonds with an increasing of the X-site cation charge.

This was tested on tourmaline samples from [52] of the fluor-elbaite–fluor-liddicoatite solid solution [52] (Figure 9). An increase of the X-site charge results in the significant shortening of X–O2 bonds. However, X–O4 and X–O5 did not show any significant correlation of the bond length to the X-site charge. Consequently, the main change in the distribution of the bond valence is located at the X–O2 bonds connecting the X site with the YO_6 octahedra. In contrast, the length of the Y–O2 bonds increase, indicating a reduction of the bond valence. This is consistent with the structural graph calculations.

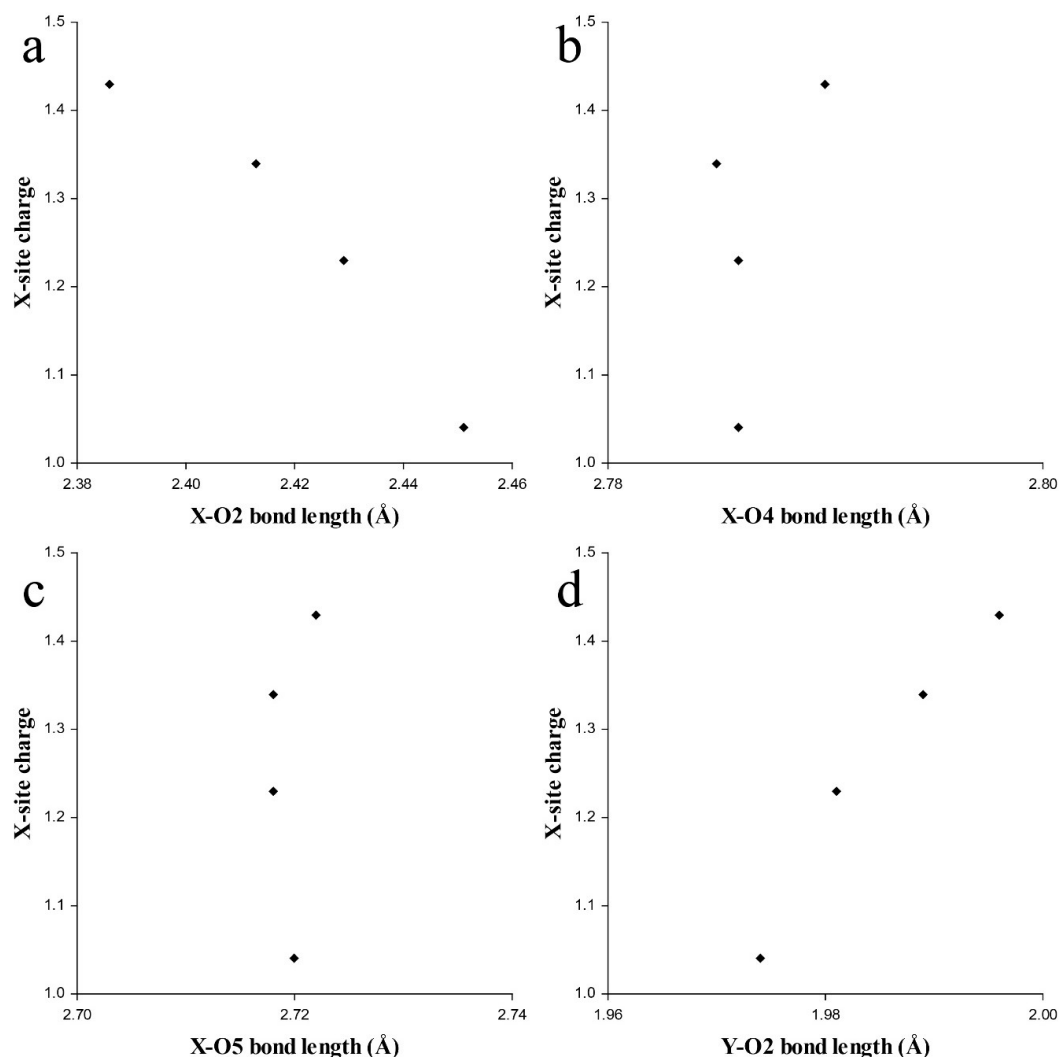


Figure 9. Correlation between the average X-site charge (Na¹⁺, Ca²⁺, K¹⁺) to (a) X–O2, (b) X–O4, (c) X–O5 and (d) Y–O2 bond lengths in tourmalines with varying fluor-elbaite and fluor-liddicoatite components [52]. The standard deviation of the bond lengths is within the size of the symbols.

3.2. Pb⁴⁺ and Bi⁵⁺ at the Octahedral Sites

The possibility of a Pb⁴⁺ and Bi⁵⁺ substitution at the octahedral sites can be tested similarly to the X-site substitutions. The Pb⁴⁺–O and Bi⁵⁺–O bond lengths calculated for the octahedral coordination are similar to the Fe²⁺–O bond length (2.1536 Å), while the Al³⁺–O bond is significantly shorter (1.9043 Å, [45]). Consequently, we presume that Pb⁴⁺ and Bi⁵⁺ would prefer the larger Y site.

The primary arrangement is the same as for the X-site substitution — Cu-bearing fluor-elbaite (Figures 10a and 11a). The procedure of attaching the bond valences to the topological graph edges was the same.

The Pb and Bi substitutions provide a larger variability in substitution mechanism allowing high-charged cations at the Y site. The Pb⁴⁺ substitutions at the Y site include (1) Pb⁴⁺ Li¹⁺ (Al³⁺ Cu²⁺)_{–1} (Figure 10b), (2) Pb⁴⁺ □ (Al³⁺ Na¹⁺)_{–1} (Figure 10c), (3) Pb⁴⁺ V O^{2–} (Al³⁺ V OH[–])_{–1} (Figure 10d). In the arrangement of the first substitution, the presence of Pb⁴⁺-neighboring 2 Li¹⁺ cations produces very small Na–O2 and Li–O2 bond valences and, consequently, it would either not be very stable or would produce a quite large structural strain. The second substitution also results in relatively small bond valences in the neighboring sites, but the Li–O bond valence of 0.08 vu is closer to the stable value than the Cu²⁺–O2 bond valence. Most stable is the third arrangement with O at the V site. A similar

arrangement with OH at the V site and ^WO instead of ^WF produces negative bond valences at the neighboring sites and therefore would not be possible.

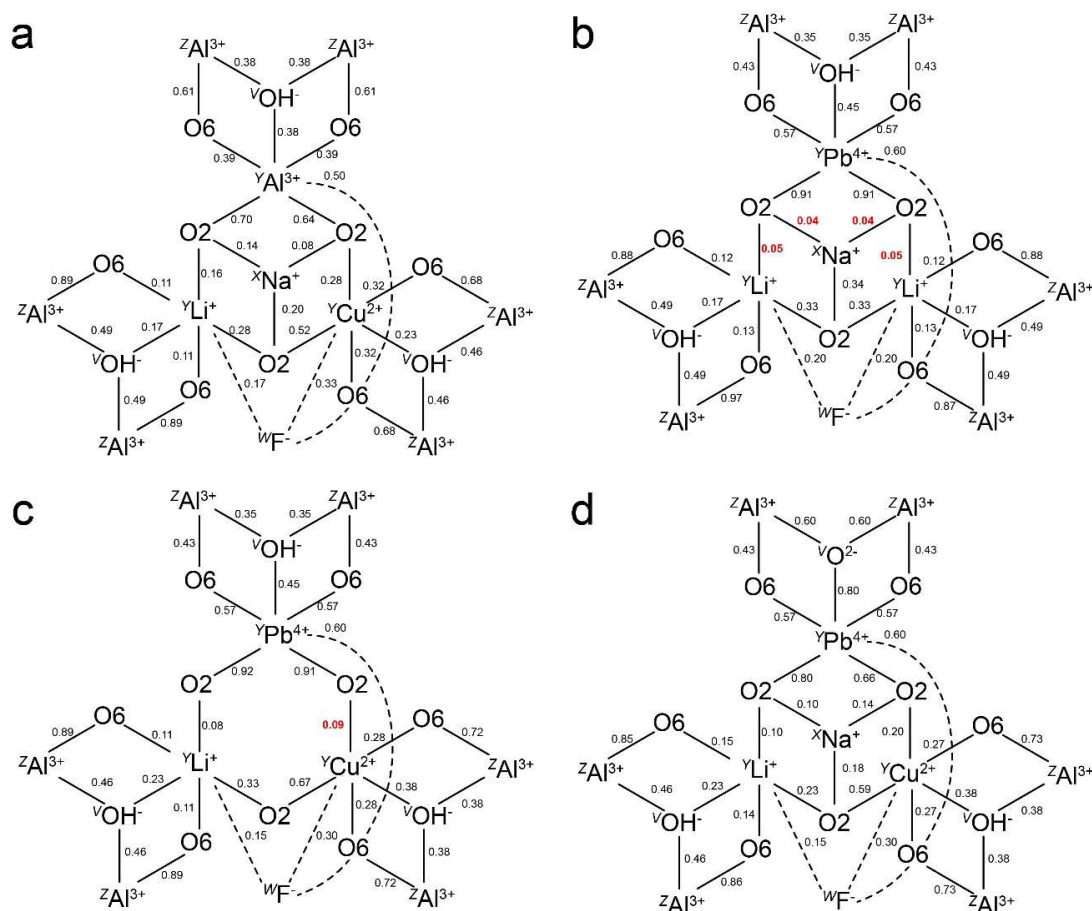


Figure 10. Structural arrangement graphs of the Y-site neighborhood in the structure of (a) Cu-bearing elbaite and arrangements derived by (b) Pb⁴⁺ Li⁺ (Al³⁺ Cu²⁺)₋₁, (c) Pb⁴⁺ □ (Al³⁺ Na⁺)₋₁ and (d) Pb⁴⁺ VO₂⁻ (Al³⁺ VOH⁻)₋₁ substitutions. The values in red color indicate very low bond valences, which do not seem to be stable.

The Bi⁵⁺ substitution at the Y site is even more challenging due to the larger difference in charge compared to the usual cations occupying this site in such a tourmaline. The difference of two charges compared to Al³⁺, 3 charges to Cu²⁺, and four charges to Li⁺ suggests that natural solutions for the substitution should involve Al³⁺. Consequently, three possible mechanisms were derived from the structural arrangement of Cu-bearing fluor-elbaite (Figure 11a): (1) Bi⁵⁺ Li⁺ VO₂⁻ (Al³⁺ Cu²⁺ WF⁻)₋₁ (Figure 11b), (2) Bi⁵⁺ □ VO₂⁻ (Al³⁺ Na⁺ WF⁻)₋₁ (Figure 11c), (3) Bi⁵⁺ Li⁺ VO₂⁻ VOH⁻ (Al³⁺ Cu²⁺ VOH⁻ WF⁻)₋₁ (Figure 11d). All structural arrangements produce unacceptably high bond valences at the Bi⁵⁺–O₂ bonds, which are unlikely to be compensated through distributing of bond valence to the neighboring sites (Z, B), which are occupied by relatively high-charged elements (Al³⁺, B³⁺) with a relatively small bond valence variability. Consequently, Bi⁵⁺ would not be stable at the Y site in any structural arrangement derived from Cu-bearing fluor-elbaite.

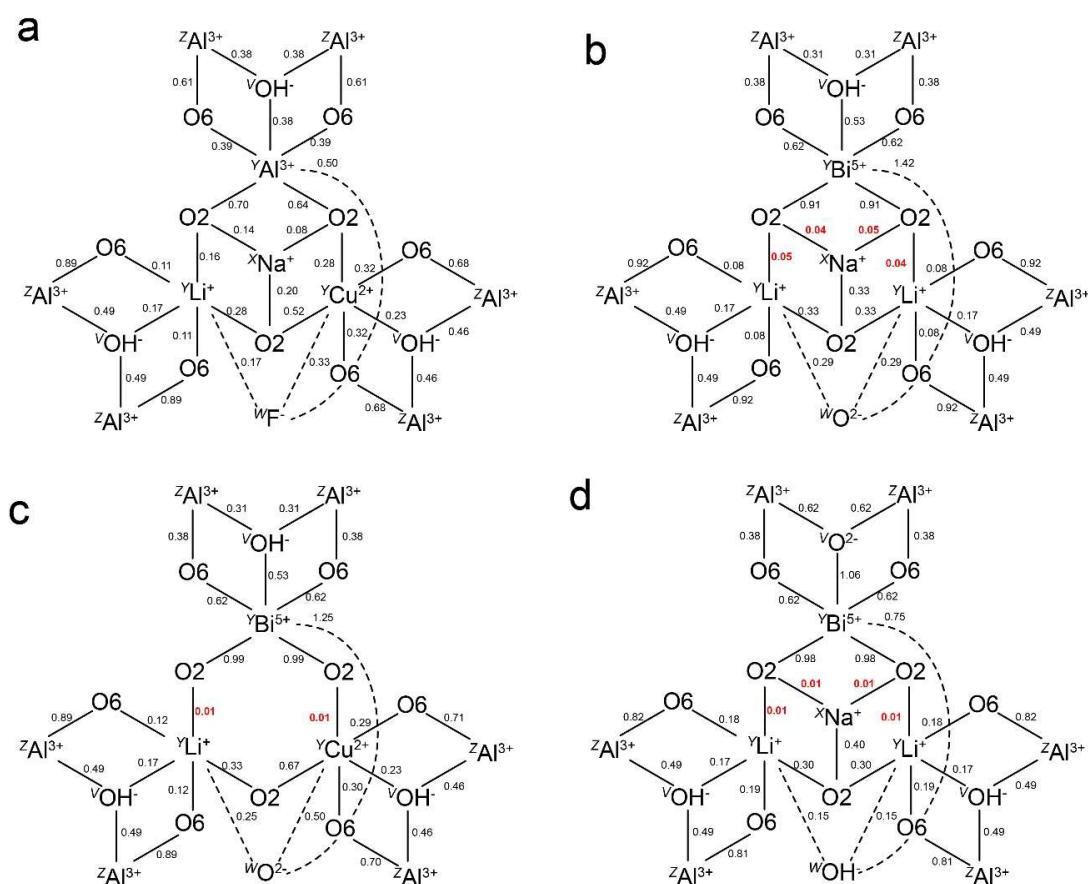


Figure 11. Structural arrangement graphs of the Y-site neighborhood in the structure of (a) Cu-bearing elbaite and arrangements derived from it by (b) $\text{Bi}^{5+} \text{Li}^{1+} \text{WO}_2^- (\text{Al}^{3+} \text{Cu}^{2+} \text{WF}^-)_{-1}$, (c) $\text{Bi}^{5+} \square \text{WO}_2^- (\text{Al}^{3+} \text{Na}^{1+} \text{WF}^-)_{-1}$, (d) $\text{Bi}^{5+} \text{Li}^{1+} \text{VO}_2^- \text{WOH}^- (\text{Al}^{3+} \text{Cu}^{2+} \text{VOH}^- \text{WF}^-)_{-1}$ substitutions. The values in red color indicate bond valences, which do not seem to be stable.

However, if we consider the Bi^{5+} substitution at the Y site in completely different structural arrangements, it can be stable at specific conditions. In an arrangement derived from Al-Mg disordered dravite (Figure 12a) Bi^{5+} can be introduced to the Y site by the substitution $\text{Bi}^{5+} \square \text{VO}_2^- \text{WO}_2^- (\text{Mg}^{2+} \text{Na}^{1+} \text{VOH}^- \text{WOH}^-)_{-1}$ (Figure 12b). This substitution produces reasonable bond valences, although relatively low Al–O2 and Mg–O2 bond valences would result in structural strain. If this arrangement is locally present in a fluor-elbaite crystal, it can allow the incorporation of Bi^{5+} into the structure. However, it would require a highly oxidative environment together with some amounts of Mg. This is not very likely, because usually Mg is at the detection limit in elbaite tourmalines.

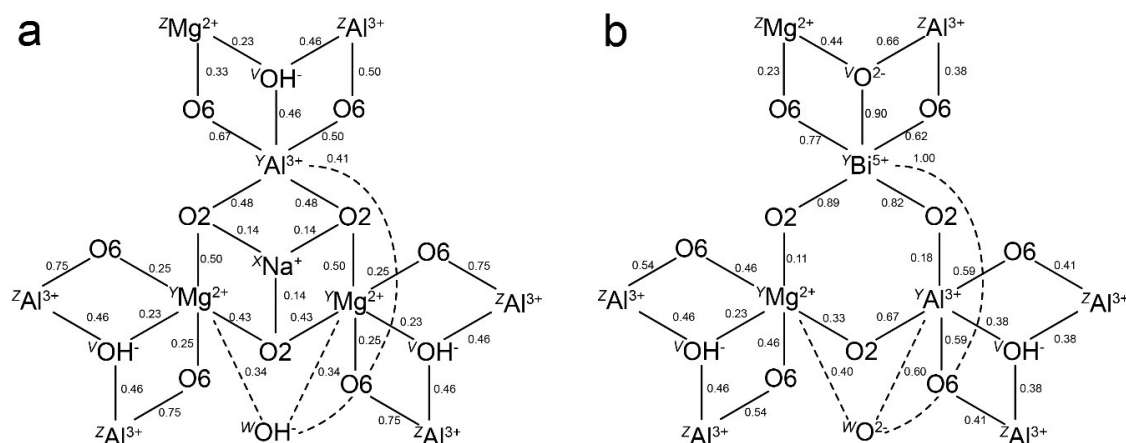


Figure 12. Structural arrangement graph of the Y-site neighborhood in the structure of (a) Al-Mg disordered dravite and (b) an arrangement derived from it by $\text{Bi}^{5+} \square \text{VO}_2^- \text{WO}_2^- (\text{Mg}^{2+} \text{Na}^{1+} \text{VOH}^- \text{WOH}^-)_{-1}$ substitution.

4. Discussion

Based on published data and the effective ionic radius, it seems that Pb usually occupies as Pb^{2+} the X site in tourmaline. This is in agreement when plotting the X-site charge (including Pb^{2+}) against the F content in Pb-rich tourmaline samples from the Minh Tien pegmatite in Vietnam. Although only limited data about the contents of Bi and Pb in “Paraíba tourmaline” (Cu- and Mn-bearing tourmaline) are available, we plotted the data of two localities in the Rio Grande do Norte State, Brazil. The correlation (between the X-site charge and F content) by using tourmaline samples from the Alto dos Quintos mine with almost no Pb, but small amounts of Bi, gets better, when Bi^{3+} is considered to occupy the X site. Bond valence calculations (3.1.) have shown that it is possible for Pb^{2+} and Bi^{3+} to occupy the X site.

Contrary to the samples from the Alto dos Quintos mine the correlation by using tourmaline samples from the Mulungu mine (Capoeira 2 pegmatite) is getting worse when Pb^{2+} and Bi^{3+} were considered to occupy the X site. Can this be an indication that Pb and Bi do not occupy the X site at that locality? Is it theoretically possible that small amounts of Pb^{4+} and Bi^{5+} occupy the Y site? Based on their effective ionic radii, it is theoretically possible. However, bond valence calculations show that there are only stable structural arrangements (derived from Cu-bearing elbaitic tourmaline) for Pb^{4+} and not for Bi^{5+} at the Y site. Although Pb^{4+} might occupy the Y site, a highly oxidative environment would be required.

In a mafic eclogite, a Sr-rich high-pressure tourmaline was described, where the authors suggested that small amounts of Pb^{4+} occupy the Y site [36]. They argue that because ~80% of the total Fe is oxidized to Fe^{3+} it is likely that Pb is also oxidized to Pb^{4+} in such an oxidative environment. A recent XAFS study of Cu-bearing tourmaline from one of the pegmatites (Alto dos Quintos mine, Pitombeira pegmatite) in the Rio Grande do Norte State, has shown that 40% of the total Mn in this Cu-bearing tourmaline was oxidized to Mn^{3+} . No native Cu (as inclusions in Cu-bearing tourmaline) was described from this pegmatite (Alto dos Quintos mine), as was described from the first locality for Cu-bearing tourmaline in São José da Batalha in the neighbor state Paraíba [53]. Instead, the occurrence of magnetite was described [54]. From the Mulungu mine was the occurrence of gahnite (inclusions in feldspar) described [54], but also no native Cu. However, it is still not clear if the pegmatite at the Mulungu mine was indeed oxidative enough for the occurrence of Pb^{4+} .

Another explanation for the abovedescribed correlation of the Mulungu mine samples could be that the amounts of Bi and Pb varied significantly during the crystallization stage, which means that during the tourmaline crystallization some additional Bi and Pb came into the pegmatitic system and hence disturbed the correlation between the average X-site charge and the F content.

We conclude that more chemical data (including F) of such Cu-bearing elbaitic tourmaline samples with significant amounts of Pb and Bi from different localities is necessary to plot more correlations.

Mössbauer studies of Fe-bearing “Paraíba tourmaline” samples would also be helpful to learn more about the oxidation states of Fe in these pegmatites to verify or falsify that these pegmatites represent an oxidative environment. Such investigations could help answering the question from where and when these uncommon elements in tourmaline (Cu, Bi, Pb) were derived. Further plots of correlations between the X-site charge and F content in such “Paraíba tourmaline” samples might also be helpful to distinguish between the worldwide localities of these rare and sought-after tourmalines.

Author Contributions: Conceptualization, A.E. and P.B.; correlation analysis, A.E.; bond valence calculations, P.B.; writing, A.E., P.B. All authors have read and agreed to the published version of the manuscript.

Funding: This work was supported by the Austrian Science Fund (FWF) project no. P 31049-N29 (AE) and by the Slovak Research and Development Agency under the Contract no. APVV-18-0065 (PB).

Acknowledgments: We are thankful to Jan Cempírek, Brno, Czech Republic, and George R. Rossman, Pasadena, USA, for providing us with references and for discussions. The constructive reviews of two anonymous reviewers improved this work significantly. Thanks for Open Access Funding by the Austrian Science Fund (FWF). Last but not least, we would like to thank Katharina Winand, Vienna, Austria, for improving our English language.

Conflicts of Interest: The authors declare no conflict of interest.

References

1. Povondra, P.; Čech, A. A method for the chemical analysis of tourmaline. *Acta Univ. Carol. Geol.* **1976**, *1976*, 209–218.
2. Foit, F.F.; Rosenberg, P.E. The structure of vanadium-bearing tourmaline and its implications regarding tourmaline solid solutions. *Am. Mineral.* **1979**, *64*, 788–798.
3. Deer, W.A.; Howie, R.A.; Zussman, J. *Rock-Forming Minerals. Vol. 1B: Disilicates and Ring Silicates*, 2nd ed.; Longman, Burnt Mill: Harlow, UK, 1986.
4. Foit, F.F. Crystal chemistry of alkali-deficient schorl and tourmaline structural relationships. *Am. Mineral.* **1989**, *74*, 422–431.
5. Hawthorne, F.C.; MacDonald, D.J.; Burns, P.C. Reassignment of cation site occupancies in tourmaline: Al-Mg disorder in the crystal structure of dravite. *Am. Mineral.* **1993**, *78*, 265–270.
6. MacDonald, D.J.; Hawthorne, F.C. The crystal chemistry of Si = Al substitution in tourmaline. *Can. Mineral.* **1995**, *33*, 849–858.
7. Hawthorne, F.C. Structural mechanisms for light-element variations in tourmaline. *Can. Mineral.* **1996**, *34*, 123–132.
8. Henry, D.J.; Dutrow, B.L. Metamorphic Tourmaline and Its Petrologic Applications. *Rev. Mineral.* **1996**, *33*, 503–557.
9. Ertl, A.; Pertlik, F.; Bernhardt, H.-J. Investigations on Olenite with Excess Boron from the Koralpe, Styria, Austria. *Österr. Akad. Wiss. Math. Naturwiss. Kl. Abt. I Anz.* **1997**, *6*, 3–10.
10. Ertl, A.; Kolitsch, U.; Dyar, M.D.; Hughes, J.M.; Rossman, G.R.; Pieczka, A.; Henry, D.J.; Pezzotta, F.; Prowatke, S.; Lengauer, C.L.; et al. Limitations of Fe²⁺ and Mn²⁺ site occupancy in tourmaline: Evidence from Fe²⁺- and Mn²⁺-rich tourmaline. *Am. Mineral.* **2012**, *97*, 1402–1416. [[CrossRef](#)]
11. Ertl, A.; Tillmanns, E. The [9]-coordinated X site in the crystal structure of tourmaline-group minerals. *Z. Krist.* **2012**, *227*, 456–459. [[CrossRef](#)]
12. Ertl, A.; Schuster, R.; Hughes, J.M.; Ludwig, T.; Meyer, H.-P.; Finger, F.; Dyar, M.D.; Ruschel, K.; Rossman, G.R.; Klötzli, U.; et al. Li-bearing tourmalines in Variscan granitic pegmatites from the Moldanubian nappes, Lower Austria. *Eur. J. Mineral.* **2012**, *24*, 695–715. [[CrossRef](#)]
13. Hawthorne, F.C.; Henry, D.J. Classification of the minerals of the tourmaline group. *Eur. J. Mineral.* **1999**, *11*, 201–216. [[CrossRef](#)]
14. Bosi, F.; Lucchesi, S. Crystal chemistry of the schorl-dravite series. *Eur. J. Mineral.* **2004**, *16*, 335–344. [[CrossRef](#)]
15. Bosi, F.; Lucchesi, S.; Reznitskii, L. Crystal chemistry of the dravite-chromdravite series. *Eur. J. Mineral.* **2004**, *16*, 345–352. [[CrossRef](#)]
16. Bosi, F.; Andreozzi, G.B.; Federico, M.; Graziani, G.; Lucchesi, S. Crystal chemistry of the elbaite-schorl series. *Am. Mineral.* **2005**, *90*, 1784–1792. [[CrossRef](#)]

17. Henry, D.J.; Novák, M.; Hawthorne, F.C.; Ertl, A.; Dutrow, B.L.; Uher, P.; Pezzotta, F. Nomenclature of the tourmaline-super group minerals. *Am. Mineral.* **2011**, *96*, 895–913. [CrossRef]
18. Vereshchagin, O.S.; Rozhdestvenskaya, I.V.; Frank-Kamenetskaya, O.V.; Zolotarev, A.A.; Mashkovtsev, R.I. Crystal chemistry of Cu-bearing tourmalines. *Am. Mineral.* **2013**, *98*, 1610–1616. [CrossRef]
19. Vereshchagin, O.S.; Frank-Kamenetskaya, O.V.; Rozhdestvenskaya, I.V. Crystal structure and stability of Ni-rich synthetic tourmaline. Distribution of divalent transition-metal cations over octahedral positions. *Mineral. Mag.* **2015**, *79*, 997–1006. [CrossRef]
20. Bačík, P.; Koděra, P.; Uher, P.; Ozdín, D.; Jánošík, M. Chlorine-enriched tourmalines in hydrothermally altered diorite porphyry from the Biely vrch porphyry gold deposit (Slovakia). *Can. Mineral.* **2015**, *53*, 673–691. [CrossRef]
21. MacDonald, D.J.; Hawthorne, F.C. Cu-bearing tourmaline from Paraiba, Brazil. *Acta Crystallogr. Sect. C Cryst. Struct. Commun.* **1995**, *51*, 555–557. [CrossRef]
22. Ertl, A.; Hughes, J.M.; Brandstätter, F. Structural and Chemical Data of Cu-bearing elbaite from Alto dos Quintos mine, Brazil. 2002. Available online: [http://members.a1.net/andreas.ertl/elbaite\(Cu\)_add_data.pdf](http://members.a1.net/andreas.ertl/elbaite(Cu)_add_data.pdf) (accessed on 29 May 2020).
23. Ertl, A.; Vereshchagin, O.S.; Giester, G.; Tillmanns, E.; Meyer, H.-P.P.; Ludwig, T.; Rozhdestvenskaya, I.V.; Frank-Kamenetskaya, O.V. Structural and chemical investigation of a zoned synthetic Cu-rich tourmaline. *Can. Mineral.* **2015**, *53*, 209–220. [CrossRef]
24. Ertl, A.; Hughes, J.M.; Prowatke, S.; Ludwig, T.; Brandstätter, F.; Körner, W.; Dyar, M.D. Tetrahedrally coordinated boron in Li-bearing olenite from “mushroom” tourmaline from Momeik, Myanmar. *Can. Mineral.* **2007**, *45*, 891–899. [CrossRef]
25. Fritsch, E.; Shigley, J.E.; Rossman, G.R.; Mercer, M.E.; Muhlmeister, S.M.; Moon, M. Gem-quality cuprian tourmalines from São José da Batalha in Paraiba, Brazil. *Gems Gemol.* **1990**, *26*, 189–205. [CrossRef]
26. Shigley, J.E.; Cook, B.C.; Laurs, B.M.; De Bernardes, M.O. An update on “Paraíba” tourmaline from Brazil. *Gems Gemol.* **2001**, *37*, 260–276. [CrossRef]
27. Milisenda, C.C. “Paraíba-Tourmaline” aus Quintos de Baixo, Rio Grande do Norte, Brasilien. *Z. Dt. Gemmol. Ges.* **2005**, *54*, 73–84.
28. Okrusch, M.; Ertl, A.; Schüssler, U.; Tillmanns, E.; Brätz, H.; Bank, H. Major- and trace-element composition of Paraíba-type Tourmaline from Brazil, Mozambique and Nigeria. *J. Gemmol.* **2016**, *35*, 120–139. [CrossRef]
29. Abduriyim, A.; Kitawaki, H.; Furuya, M.; Schwarz, D. “Paraíba”-type copper-bearing tourmaline from Brazil, Nigeria, and Mozambique: Chemical fingerprinting by LA-ICP-MS. *Gems Gemol.* **2006**, *42*, 4–21. [CrossRef]
30. Johnson, M.L.; Wentzell, C.Y.; Elen, S. Multicolored bismuth-bearing tourmaline from Lundazi, Zambia. *Gems Gemol.* **1997**, *33*, 204–211. [CrossRef]
31. Lussier, A.J.; Abdu, Y.; Hawthorne, F.C.; Michaelis, V.K.; Aguiar, P.M.; Kroekennr, S. Oscillatory zoned liddicoatite from Anjanaboina, Central Madagascar. I. Crystal chemistry and structure by SREF and ¹¹B and ²⁷Al MAS NMR spectroscopy. *Can. Mineral.* **2011**, *49*, 63–88. [CrossRef]
32. Sokolov, M.; Martin, R.F. A Pb-dominant member of the tourmaline group, Minh Tien granitic pegmatite, Luc Yen district, Vietnam. *Estud. Geol.* **2009**, *19*, 352–353.
33. Kubernátová, M. *Composition of Pb-Rich Tourmaline from the Pegmatite Minh Tien, Vietnam*; Masaryk University: Brno, Czech Republic, 2019.
34. Kubernátová, M.; Cempírek, J. Crystal chemistry of Pb-rich tourmaline from pegmatite in Minh Tien, Vietnam. In Proceedings of the 9th European Conference on Mineralogy and Spectroscopy, Prague, Czech Republic, 11–13 September 2019.
35. Henry, D.J. Fluorine—X-site vacancy avoidance in natural tourmaline: Internal vs external control. In Proceedings of the 2005 Goldschmidt Conference, Moscow, ID, USA, 20–25 May 2005; p. 1318.
36. Ertl, A.; Kolitsch, U.; Meyer, H.P.; Ludwig, T.; Lengauer, C.L.; Nasdala, L.; Tillmanns, E. Substitution mechanism in tourmalines of the “Fluor-Elbaite”-rossmanite series from Wolkenburg, Saxony, Germany. *Neues Jahrb. Mineral. Abh.* **2009**, *186*, 51–61. [CrossRef]
37. Ertl, A.; Rossman, G.R.; Hughes, J.M.; London, D.; Wang, Y.; O’Leary, J.A.; Dyar, M.D.; Prowatke, S.; Ludwig, T.; Tillmanns, E. Tourmaline of the elbaite-schorl series from the Himalaya Mine, Mesa Grande, California: A detailed investigation. *Am. Mineral.* **2010**, *95*, 24–40. [CrossRef]
38. Shriver, D.F.; Atkins, P.W. *Inorganic Chemistry*, 3rd ed.; Oxford University Press: Oxford, UK, 1999.

39. Sadler, P.J.; Li, H.; Sun, H. Coordination chemistry of metals in medicine: Target sites for bismuth. *Coord. Chem. Rev.* **1999**, *185*, 689–709. [[CrossRef](#)]
40. Shannon, R.D. Revised effective ionic radii and systematic studies of interatomic distances in halides and chalcogenides. *Acta Crystallogr. Sect. A* **1976**, *32*, 751–767. [[CrossRef](#)]
41. Ertl, A.; Hughes, J.M.; Pertlik, F.; Foit, F.F.; Wright, S.E.; Brandstätter, F.; Marler, B. Polyhedron distortions in tourmaline. *Can. Mineral.* **2002**, *40*, 153–162. [[CrossRef](#)]
42. Sugiyama, K.; Arima, H.; Konno, H.; Mikouchi, T. XAFS study on the location of Cu and Mn in a greenish blue elbaite from Alto dos Quntos mine, Brazil. *J. Mineral. Pet. Sci.* **2017**, *112*, 139–146. [[CrossRef](#)]
43. Brown, I.D. *The Chemical Bond in Inorganic Chemistry: The Bond Valence Model*; Oxford University Press: Oxford, UK, 2010; ISBN 9780191708879.
44. Gagné, O.C.; Hawthorne, F.C. Comprehensive derivation of bond-valence parameters for ion pairs involving oxygen. *Acta Crystallogr. Sect. B Struct. Sci. Cryst. Eng. Mater.* **2015**, *71*, 562–578. [[CrossRef](#)]
45. Bačík, P.; Fridrichová, J. Cation partitioning among crystallographic sites based on bond-length constraints in tourmaline-supergroup minerals. *Am. Mineral.* **2020**, *96*, 895–913.
46. Hawthorne, F.C. Bond-valence constraints on the chemical composition of tourmaline. *Can. Mineral.* **2002**, *40*, 789–797. [[CrossRef](#)]
47. Bosi, F. Stereochemical constraints in tourmaline: From a short-range to a long-range structure. *Can. Mineral.* **2011**, *49*, 17–27. [[CrossRef](#)]
48. Bačík, P. Cation ordering at octahedral sites in schorl-dravite series tourmalines. *Can. Mineral.* **2015**, *53*, 571–590. [[CrossRef](#)]
49. Bačík, P. The crystal-chemical autopsy of octahedral sites in Na-dominant tourmalines: Octahedral metrics model unconstrained by the Y,Z-site disorder assignment. *J. Geosci. (Czech Repub.)* **2018**, *63*, 137–154. [[CrossRef](#)]
50. Ertl, A.; Kolitsch, U.; Prowatke, S.; Dyar, M.D.; Henry, D.J. The F-analogue of schorl from Grasstein, Trentino South Tyrol, Italy: Crystal structure and chemistry. *Eur. J. Mineral.* **2006**, *18*, 583–588. [[CrossRef](#)]
51. Ertl, A.; Giester, G.; Ludwig, T.; Meyer, H.P.; Rossman, G.R. Synthetic B-rich olenite: Correlations of single-crystal structural data. *Am. Mineral.* **2012**, *97*, 1591–1597. [[CrossRef](#)]
52. Ertl, A.; Hughes, J.M.; Prowatke, S.; Ludwig, T.; Prasad, P.S.R.; Brandstätter, F.; Körner, W.; Schuster, R.; Pertlik, F.; Marschall, H. Tetrahedrally coordinated boron in tourmalines from the liddicoatite-elbaite series from Madagascar: Structure, chemistry, and infrared spectroscopic studies. *Am. Mineral.* **2006**, *91*, 1847–1856. [[CrossRef](#)]
53. Brandstätter, F.; Niedermayr, G. Einschlüsse von ged. Kupfer im Cu-Elbait von São José da Batalha in Paraíba, Brasilien. *Z. Dt. Gemmol. Ges.* **1993**, *42*, 37–41.
54. Beurlen, H.; Müller, A.; Silva, D.; Da Silva, M.R.R. Petrogenetic significance of LA-ICP-MS trace-element data on quartz from the Borborema Pegmatite Province, northeast Brazil. *Mineral. Mag.* **2011**, *75*, 2703–2719. [[CrossRef](#)]



© 2020 by the authors. Licensee MDPI, Basel, Switzerland. This article is an open access article distributed under the terms and conditions of the Creative Commons Attribution (CC BY) license (<http://creativecommons.org/licenses/by/4.0/>).